

Controlling blue-violet electroluminescence of Ge-rich Er-doped SiO₂ layers by millisecond annealing using flash lamps

A. Kanjilal, L. Rebohle, M. Voelskow, M. Helm, and W. Skorupa

Citation: *Journal of Applied Physics* **107**, 023114 (2010); doi: 10.1063/1.3296252

View online: <http://dx.doi.org/10.1063/1.3296252>

View Table of Contents: <http://scitation.aip.org/content/aip/journal/jap/107/2?ver=pdfcov>

Published by the [AIP Publishing](#)

Articles you may be interested in

Comparison of the room temperature 1.53 μm Er photoluminescence from flash lamp and furnace annealed Er-doped Ge-rich SiO₂ layers

J. Appl. Phys. **107**, 113523 (2010); 10.1063/1.3437652

The role of Ge-related oxygen-deficiency centers in controlling the blue-violet photo- and electroluminescence in Ge-rich SiO₂ via Er doping

J. Appl. Phys. **106**, 063112 (2009); 10.1063/1.3225911

Defect-engineered blue-violet electroluminescence from Ge nanocrystal rich SiO₂ layers by Er doping

J. Appl. Phys. **106**, 026104 (2009); 10.1063/1.3183904

Fourfold increase of the ultraviolet (314 nm) electroluminescence from SiO₂:Gd layers by fluorine coimplantation and flash lamp annealing

Appl. Phys. Lett. **91**, 181107 (2007); 10.1063/1.2803855

Light emission and charge trapping in Er-doped silicon dioxide films containing silicon nanocrystals

Appl. Phys. Lett. **86**, 151914 (2005); 10.1063/1.1872208



Controlling blue-violet electroluminescence of Ge-rich Er-doped SiO₂ layers by millisecond annealing using flash lamps

A. Kanjilal,^{a)} L. Rebohle, M. Voelskow, M. Helm, and W. Skorupa

Institute of Ion Beam Physics and Materials Research, Forschungszentrum Dresden Rossendorf, P.O. Box 510119, 01314 Dresden, Germany

(Received 30 September 2009; accepted 15 December 2009; published online 29 January 2010)

Systematic evolution of the 400 nm electroluminescence (EL) with increasing flash lamp annealing (FLA) temperature from 800 to 1100 °C in an Er-doped Ge-rich metal-oxide semiconductor structure is presented. No significant change in the 1535 nm Er EL is observed with increasing FLA temperature. Enhancement of the 400 nm EL decay time with rising FLA temperature is found to be associated with recrystallization of the damaged Ge clusters in the absence of Ge outdiffusion. The 400 nm EL quenching with continuous charge injection process is also discussed within the device operation time. © 2010 American Institute of Physics. [doi:10.1063/1.3296252]

I. INTRODUCTION

The *inverse energy transfer* (IET) process that describes an electrically driven energy transfer mechanism from the Er³⁺ to the Ge-related oxygen-deficiency centers (GeODCs) in an Er-doped Ge nanocrystal (NC) enriched SiO₂ layer of a metal-oxide semiconductor structure and its corresponding impact on the blue-violet electroluminescence (EL) have recently been demonstrated.¹ The basic mechanism in such system relies on the close proximity of the Er³⁺ to the GeODCs situated mainly at the NC/SiO₂ interface.^{2,3} Since the existence of GeODCs is strongly associated with the crystalline quality of Ge nanoclusters, the control over corresponding microstructure plays an important role for achieving the highest EL.² To improve the structure of Er-doped Ge NCs, postimplantation annealing is an inevitable step. In fact, evolution of phases like Er₂O₃ or Er₂Ge₂O₇ have been realized during furnace annealing in the temperature range of 800–1100 °C for a fixed Ge and Er concentration.³ A monotonic quenching of the blue-violet EL intensity was, however, observed due to the formation of such Er composites together with a steady increase in Ge diffusion toward the SiO₂/Si and Si-oxynitride/Si (SiON/Si) interfaces.³ The question is how to control the detrimental 400 nm EL quenching by suppressing the decrease in surface-to-volume ratio of Ge NCs and/or outdiffusion of Er from the surface of Ge NCs.^{3,4}

In this context, flash lamp annealing (FLA) is challenging and promising to avoid strong diffusion and clustering of impurities in SiO₂ (Ref. 5) where such annealing process is often performed by using an extremely short temperature pulse (generally in the millisecond range⁶). Using this extraordinary approach, we present recrystallization of the Er doping induced amorphized Ge nanoclusters in the absence of Ge outdiffusion with reduced thermal budget (*viz.* annealing time) and the corresponding enhancement of the 400 nm EL intensity. Moreover, we show that the 400 nm EL intensity and its decay time increase systematically with increasing FLA temperature without changing the 1535 nm Er EL

yield. We will also show that, for a constant current, the 400 nm EL intensity quenches with device operation time where the quenching mechanism is strongly associated with the FLA temperature.

II. EXPERIMENTAL

Initially, 130 keV Ge ions were implanted with a dose of 4×10^{16} cm⁻², which gives 7.4% Ge at the mean projected range R_p of ~ 112 nm (derived from the SRIM-2006 calculations⁷) into a 200 nm thick thermally grown SiO₂ layer with a local oxidation of Si (LOCOS) structure on *n*-type Si(100) wafer. The samples were subjected to FLA for 20 ms at 1050 °C with an additional preheating at ~ 700 °C to produce small Ge NCs in the range of 2–4 nm (not shown here). Subsequently, 250 keV Er ions were implanted with a dose of 2×10^{15} cm⁻² giving $\sim 0.5\%$ Er at $R_p \sim 115$ nm, followed by FLA for 20 ms with temperature in between 800 and 1100 °C to remove implantation-induced defects and for activating Er³⁺ ions. The Ge and Er concentrations were further verified by Rutherford backscattering spectrometry (RBS) with a 1.4 MeV ⁴He⁺ beam. A 100 nm thick SiON layer was deposited on top of the LOCOS structure. Moreover, semitransparent indium-tin oxide and aluminum contacts were sputter deposited on the front and rear surfaces, respectively. The top layer was further patterned by optical lithography to achieve arrays of circular electrodes with diameter of ~ 300 μm. Cross-sectional transmission-electron-microscopy images were taken by a FEI Titan 80–300 S/TEM instrument operating at 300 keV. All the EL spectra were recorded at room temperature (RT) with constant current mode and under forward bias conditions, and by a monochromator in combination with a photomultiplier or an InGaAs detector. The EL decay time was measured by a multichannel scalar (Stanford Research System SR430) under constant voltage pulses.

III. RESULTS AND DISCUSSION

Figure 1 displays the evolution of the 400 nm EL with increasing FLA temperature from 800 to 1100 °C in the ab-

^{a)}Electronic mail: a.kanjilal@fzd.de.

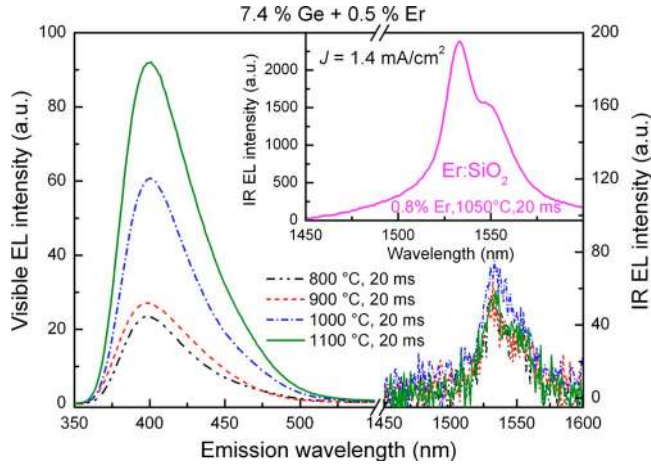


FIG. 1. (Color online) The EL spectra recorded with $J = 1.4 \text{ mA/cm}^2$ for the 7.4% Ge+0.5% Er in SiO_2 when processed by FLA with 800–1100 °C for 20 ms. The inset shows the EL spectrum of the only 0.8% Er-doped SiO_2 for $J = 1.4 \text{ mA/cm}^2$.

sence of any significant change in the 1535 nm Er EL yield for a constant current density (J) of 1.4 mA/cm^2 . In the absence of excess Ge, a strong 1535 nm Er EL can be achieved as the one shown for only 0.8% Er-doped SiO_2 (inset, Fig. 1). Using the complementary photoluminescence (PL) measurements, we have recently demonstrated⁸ these phenomena in the framework of electrically driven IET process from the Er^{3+} to the GeODCs in case of furnace annealed samples. In fact, the observed increase of the 400 nm EL intensity therefore indicates that the IET process becomes more prominent with increasing FLA temperature from 800–1100 °C (that will be discussed in the following). In contrast to the furnace annealed samples,³ no Ge outdiffusion toward the SiO_2/Si and SiON/Si interfaces was observed by RBS (Fig. 2). Please note that the Ge outdiffusion toward the Si/SiO_2 interface was even observed by RBS in rapid thermal annealed samples when they are annealed at 1050 °C for 6 s (not shown here), verifying the capability of the FLA

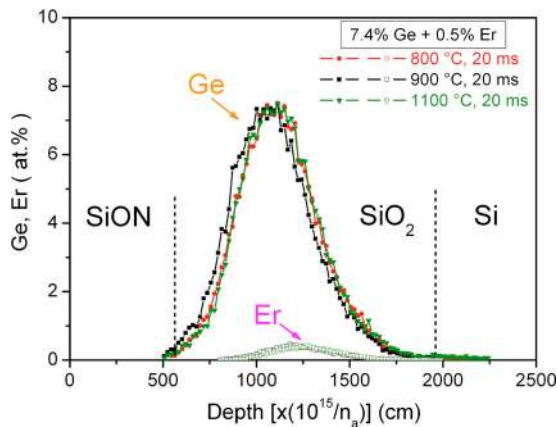


FIG. 2. (Color online) The RBS random spectra, showing the Ge (filled symbols) and Er (open symbols) profiles with increasing FLA temperature for 7.4% Ge and 0.5% Er. The dashed vertical lines represent the SiON/SiO_2 and SiO_2/Si interfaces. Taking into account the atomic densities (n_a) of 5.00×10^{22} , 6.60×10^{22} , and $6.63 \times 10^{22} \text{ at./cm}^3$ for Si, SiO_2 , and SiON , respectively, one can estimate the respective geometric layer thickness.

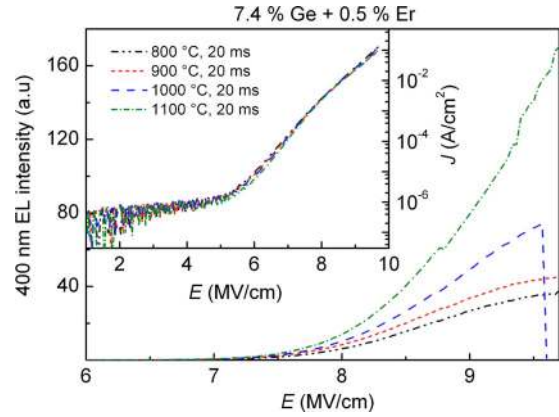


FIG. 3. (Color online) The 400 nm EL intensity vs E for the devices prepared by FLA from 800 to 1100 °C. The inset shows the corresponding J - E characteristics.

treatment to suppress Ge segregation. This is also confirmed by taking the J - E characteristics (inset, Fig. 3) into account where the E defines the applied electric field. The insignificant change in J - E profiles, especially the threshold E at different annealing temperatures implies that the barrier height at the SiO_2/Si interface is hardly affected by FLA. The charge transport from the conduction band of Si to the conduction band of SiO_2 is found to be mainly governed by the Fowler–Nordheim tunnelling.⁹ Moreover, the variation of the 400 nm EL intensity has also been examined as a function of E (Fig. 3), showing that the EL intensity is growing almost exponentially with increasing E , and the 400 nm EL intensity rises systematically with increasing annealing temperature. This phenomenon can be explained either in the light of the FLA temperature dependent improvement of the microstructure or the activation of more and more Er^{3+} ions. Since the 1535 nm EL intensity is almost unaffected with increasing FLA temperature (Fig. 1), it seems that the former one plays the key role.

The impact of FLA is more prominent if we follow both the 400 and 1535 nm EL intensities with increasing J . They were in fact monitored during J - E measurements. For the sake of our discussion, we have plotted the observed change of the 400 and 1535 nm EL intensities in Fig. 4 as a function of injected charge density ($\phi = J/q$). As apparent, the characteristic slope of the 400 nm EL intensity rises markedly with increasing FLA temperature (left panel), while no demarcating change is observed for the 1535 nm Er emission (right panel). To have an in-depth understanding, the projected curves have been fitted using a relation^{1,10} $EL = EL_{\text{max}}[\sigma\tau\phi/(\sigma\tau\phi+1)]$ where the product of the excitation cross-section (σ) and the lifetime (τ) for the 1535 nm EL is found to fluctuate between $(5.3\text{--}7.4) \times 10^{-18} \text{ cm}^2 \text{ s}$ as a function of FLA temperature, while it varies between $(11.5\text{--}4.4) \times 10^{-18} \text{ cm}^2 \text{ s}$ for the 400 nm EL peak (see the attached table, right panel in Fig. 4). It seems that the observed 1535 nm Er EL intensity is mainly associated with the Er^{3+} ions,¹ which are staying apart from Ge NCs and not taking part in IET process. Hence, we focused onto the 400 nm EL and carried out decay time (τ_d) measurements where the τ_d was estimated using a stretched exponential function¹¹ $I(t) \propto \exp[-(t/\tau_d)^\beta]$. Here, β , the dispersion factor, indicates

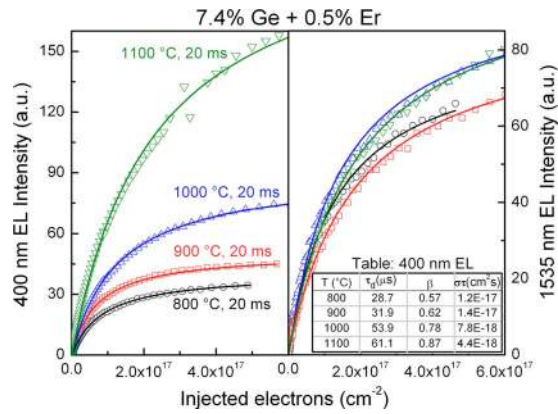


FIG. 4. (Color online) The variation of the 400 nm (left panel) and 1535 nm (right panel) EL intensities as a function of charge injection density for the devices processed by FLA with 800–1100 °C for 20 ms and superimposition of the corresponding theoretical curves. The attached table (right panel) presents the τ_d , β , and $\sigma\tau$ values of the 400 nm EL peak when the devices were processed by FLA using 800–1100 °C.

the spread of Er lifetime. The calculated τ_d values are also given in the attached table (Fig. 4), showing that both τ_d and β values are increasing as a function of FLA temperature. The corresponding σ is estimated to be of 4.0×10^{-13} , 4.4×10^{-13} , 1.5×10^{-13} , and 7.2×10^{-14} cm², respectively.

The variation of the 400 EL intensity was further examined as a function of the charge injection time for $J = 0.37$ mA/cm² (Fig. 5). From the top panel, one can see the subsequent variation of the constant current voltage (ΔV) across the electrodes, representing the *charge trapping* mechanism¹⁰ in the respective oxide matrix. As can be seen from the lower panel, although the 400 EL intensity is reduced with increasing charge injection time, the quenching

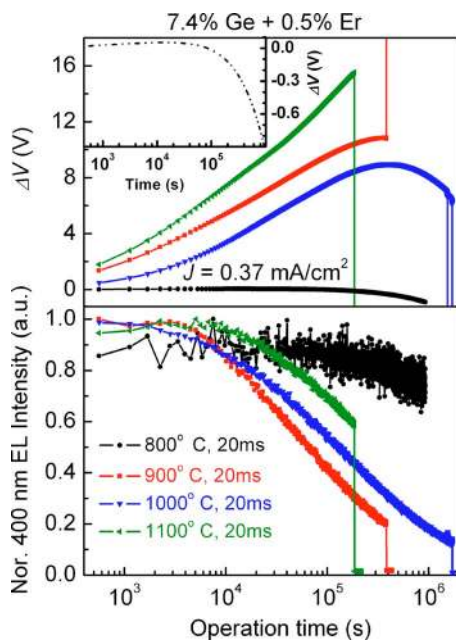


FIG. 5. (Color online) The variation of the constant current voltage (top panel) and the 400 nm EL intensity (lower panel) as a function of charge injection time, measured at $J = 0.37$ mA/cm² for the devices processed by FLA with 800–1100 °C for 20 ms. (Top panel) Inset magnifies the variation of ΔV as a function of charge injection time for the device annealed at 800 °C.

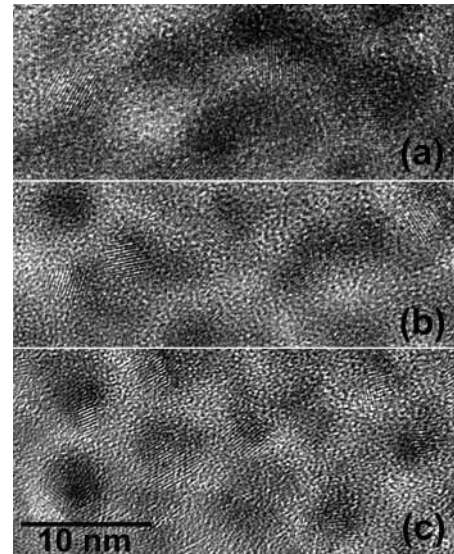


FIG. 6. The HRTEM images of the Ge-rich SiO₂ codoped with Er when processed by FLA with 800 (a), 900 (b), and 1100 °C (c) for 20 ms. All the images have the same magnification.

rate is lowest for the samples prepared by FLA at 800 °C. Conversely, the rest of the samples, which are annealed between 900 and 1100 °C, show a positive voltage shift up to $\sim 10^5$ s (Fig. 5), implying the electron trapping process. The electron trapping mechanism is found to dominate in case of the 900 and 1100 °C processed samples before reaching a catastrophic dielectric breakdown. On the other hand, both electron and hole trapping processes are observed when the samples are annealed at 1000 °C. In the latter case, the electrons are initially trapped, followed by a gradual overtaking of the hole trapping process, which is represented by the “U” turn of the curve, showing a decrease in ΔV . Note that as the dielectric breakdown is a statistical event, it is possible that the long time behavior of the ΔV characteristics for both 900 and 1100 °C is similar to that of 1000 °C. Moreover, close inspection of the curve corresponding to the sample processed at 800 °C (inset, top panel) reveals that following a weak electron trapping process up to $\sim 5 \times 10^4$ s, the hole trapping dominates.

In order to understand the charge injection mechanism, FLA dependent microstructural evolution has also been examined using high-resolution TEM (HRTEM), keeping the electron beam along the [011]-zone axis (see Fig. 6). As discerned, most of Ge NCs, damaged by Er doping, are partially recrystallized after FLA at 800 °C [Fig. 6(a)]. With increasing FLA temperatures up to 1100 °C, a systematic increase in the density of the recrystallized Ge nanoclusters is observed [Figs. 6(a)–6(c)]. Close inspection reveals that patches of gray/dark contrast are partially overlapped with Ge NCs and/or situated near Ge NCs. Although the origin of this gray/dark patches are not clear from the observed microstructures, based on our EL results (Fig. 1), it seems that they are most likely associated with the Er-rich zones. In fact, we have demonstrated earlier, for a set of furnace annealed samples,^{2,3} that the Er atoms have a tendency to passivate the surface of Ge NCs and as a consequence accelerate the IET process. A coupling between the Er³⁺ ions and the GeODCs

is essential to conduct an IET process.¹ By comparing the PL and EL results, we have also shown that the GeODCs are mainly situated at the Ge NC's surface and so the Er³⁺ ions situated near the surface of Ge NCs can only take part in IET process.⁸ Although the control over Ge distribution and the removal of implantation induced defects by FLA and furnace annealing are not comparable, the basic mechanism behind the IET process should be similar. Even if we cannot directly confirm the presence of Er-rich environment around Ge NCs by HRTEM (Fig. 6), by comparing the 1535 nm Er EL intensity (Fig. 1) for samples processed at 1000 and 1100 °C FLA in presence of excess Ge with that of only Er-doped SiO₂ (inset, Fig. 1), a strong coupling between the Er³⁺ and GeODC has to be assumed. A gradual increase of the 1535 nm Er EL intensity is expected due to the removal of the implantation induced defects with increasing FLA temperature if all Er³⁺ ions are considered to be staying isolated from the Ge-rich environment and surrounded by defects adding nonradiative channels to the Er³⁺ emission. It seems from Fig. 1 that not all but a fraction of active Er³⁺ ions are staying apart from the Ge-rich regions and remains almost unchanged at different FLA temperature. As the EL decay time of the 400 nm line increases by a factor of 2 with increasing annealing temperature from 800 to 1100 °C (Fig. 4), the decrease of nonradiative decay channels gives an equivalent contribution to the increase of the 400 nm EL intensity by a factor of 4. On the other hand, by taking into account our previous PL and EL results,⁸ one can expect an increase in density of the GeODCs due to the recrystallization of Ge clusters as a function of FLA temperature (Fig. 6). It is also possible that the GeODC-Er³⁺ coupling increases in the presence of Er near recrystallized Ge clusters. Because of this GeODC-Er³⁺ coupling which requires Er³⁺ in the close vicinity of Ge NC, the patches of gray/dark contrast in the observed microstructures (Fig. 6) are most probably due to such an Er-rich zone.

The Er ions generally trap the positive charges, while the electrons are captured in surrounding defects.¹² This processes become more efficient during EL excitation process if the Er³⁺ ions are situated close to the NC's surface.¹² Considering the impact excitation of the Er³⁺ ions, when the electrons pass through the amorphous SiO₂ layer one can expect an exchange of energy to the nearest GeODCs, which is the precondition for an IET process.¹ The probability will further improve with increasing number of Ge NCs. It seems from Fig. 5 that Ge NCs and their disordered surroundings enhance the process of electron trapping, which may subsequently induce a repulsive Coulomb scattering of the injected (*hot*) electrons above $\sim 10^4$ s leading to a significant reduction of the impact excitation process of GeODCs—thereby causing the 400 nm EL quenching. In fact, electrons usually spend a relatively long time inside the traps (either GeODCs or defects around Er³⁺) before thermalizing or tunneling to the conduction band of SiO₂ or the neighboring traps.¹³ This type of trapping/detrapping motion of carriers also reduces the electron mobilities,¹³ which in turn reduces the number of electrons that can participate in the impact excitation process.

Although the number of recrystallized Ge clusters is small in samples processed at 800 °C [Fig. 6(a)], the appearance of weak 1535 nm EL (Fig. 1) signifies that either the Er³⁺ ions reside in a Ge-rich environment² or the Er³⁺ ions are not fully activated. Since the extracted $\sigma\tau$ values of the 1535 nm Er EL are found almost identical, we can rule out the second possibility. However, the IET process demands a strong GeODC-Er³⁺ coupling,¹ which is definitely weak with such low crystalline quality of Ge clusters.² It appears that although the Er³⁺ ions can be activated by 800 °C FLA, except a few active Er³⁺ centers, most of them are possibly located near amorphized Ge nanoclusters and surrounded by a large number of nonradiative centers, leading to a weak 1535 nm Er emission. In fact, as the excitation of the higher energy levels of Er³⁺ ions¹⁴ requires higher electric field, the IET process¹ will take the lead with increasing E , in good agreement with Fig. 3. Taking into account the electron trapping in GeODCs, a gradual increase of the hole trapping mechanism beyond 5×10^4 s for the samples processed at 800 °C (inset, top panel of Fig. 5) indicates a slow transformation of the GeODCs to other types of defects¹⁰ and/or the development of stress by internal insulator field,⁹ resulting a quenching of the 400 nm EL intensity, which is rather weak compared to other flash lamp annealed samples (lower panel, Fig. 5). The situation improves with increasing recrystallization of the damaged Ge nanoclusters from 900 °C, showing a clear electron trapping¹⁰ during electron injection. The larger the density of Ge NCs surrounded by the Er³⁺, the more efficient is the screening of hot electrons. This, as a consequence, reduces the effective excitation cross-section (see Table, Fig. 4).

IV. CONCLUSIONS

In summary, we have demonstrated a gradual enhancement of the 400 nm EL intensity through promotion of the IET process via increasing the density of recrystallized Ge nanoclusters in Ge-rich Er-doped MOS structure by increasing the FLA temperature from 800 to 1100 °C. The 400 nm EL intensity was found to increase continuously, irrespective of the FLA temperature with applied electric field until dielectric breakdown, revealing that the IET process becomes more pronounced with increasing electric field. Operation time dependent quenching of the 400 nm EL is described in the light of a competition between the electron and hole trapping mechanisms, while the trapping of holes dominates over the initial electron trapping mechanism due to the transformation of the GeODCs at the Ge NC's surface via continuous injection of electrons.

ACKNOWLEDGMENTS

The authors wish to thank the Rossendorf Implantation Group for ion implantation and H. Felsmann, C. Neisser, and G. Schnabel for their careful semiconductor preparation work. This work is financially supported by the Alexander von Humboldt Foundation.

¹A. Kanjilal, L. Rebohle, M. Voelskow, W. Skorupa, and M. Helm, *Appl. Phys. Lett.* **94**, 051903 (2009).

²A. Kanjilal, L. Rebohle, M. Voelskow, W. Skorupa, and M. Helm, *J. Appl.*

- Phys.* **106**, 026104 (2009).
- ³A. Kanjilal, L. Rebohle, N. K. Baddela, S. Zhou, M. Voelskow, W. Skorupa, and M. Helm, *Phys. Rev. B* **79**, 161302(R) (2009).
- ⁴A. Kanjilal, L. Rebohle, W. Skorupa, and M. Helm, *Appl. Phys. Lett.* **94**, 101916 (2009).
- ⁵L. Rebohle, J. Lehmann, S. Prucnal, A. Kanjilal, A. Nazarov, I. Tyagulskii, W. Skorupa, and M. Helm, *Appl. Phys. Lett.* **93**, 071908 (2008).
- ⁶W. Skorupa, T. Gebel, R. A. Yankov, S. Paul, W. Lerch, D. F. Downey, and E. A. Arevalo, *J. Electrochem. Soc.* **152**, G436 (2005).
- ⁷J. F. Ziegler and J. P. Biersack, SRIM-2006.02 (<http://www.srim.org>).
- ⁸A. Kanjilal, S. Tsushima, C. Götz, L. Rebohle, M. Voelskow, W. Skorupa, and M. Helm, *J. Appl. Phys.* **106**, 063112 (2009).
- ⁹T. Hori, *Gate Dielectrics and MOS ULSIs, Principle, Technologies, and Applications* (Springer-Verlag, Berlin, 1997).
- ¹⁰A. N. Nazarov, I. N. Osiyuk, J. M. Sun, R. A. Yankov, W. Skorupa, I. P. Tyagulskii, V. S. Lysenko, S. Prucnal, T. Gebel, and L. Rebohle, *Appl. Phys. B: Lasers Opt.* **87**, 129 (2007).
- ¹¹L. Pavesi and M. Ceschini, *Phys. Rev. B* **48**, 17625 (1993).
- ¹²A. Nazarov, J. M. Sun, W. Skorupa, R. A. Yankov, I. N. Osiyuk, I. P. Tyagulskii, V. S. Lysenko, and T. Gebel, *Appl. Phys. Lett.* **86**, 151914 (2005).
- ¹³D. J. DiMaria and M. V. Fischetti, in *Excess Electrons in Dielectric Media*, edited by C. Ferradini and J. P. Jay-Gerin (CRC, Boca Raton, 1991), Chap. 10.
- ¹⁴G. H. Dieke, *Spectra and Energy Levels of Rare Earth Ions in Crystals* (Interscience Publishers, New York, 1968), Chap. 13.